The Astrophysical Journal, 633:L113–L116, 2005 November 10

FORMATION OF STRUCTURE IN MOLECULAR CLOUDS: A CASE STUDY

Fabian Heitsch,[1,2] Andreas Burkert,[1] Lee W. Hartmann,[3] Adrianne D. Slyz,[4] and Julien E. G. Devriendt[5]

Received 2005 June 7; accepted 2005 September 29; published 2005 October 26

ABSTRACT

Molecular clouds (MCs) are highly structured and turbulent. Colliding gas streams of atomic hydrogen have been suggested as a possible source of MCs, imprinting the filamentary structure as a consequence of dynamical and thermal instabilities. We present a two-dimensional numerical analysis of MC formation via converging H I flows. Even with modest flow speeds and completely uniform inflows, nonlinear density perturbations arise as possible precursors of MCs. Thus, we suggest that MCs are inevitably formed with substantial structure, e.g., strong density and velocity fluctuations, which provide the initial conditions for subsequent gravitational collapse and star formation in a variety of Galactic and extragalactic environments.

Subject headings: ISM: clouds — ISM: kinematics and dynamics — methods: numerical — stars: formation — turbulence

Online material: color figure

1. MOTIVATION

Molecular clouds (MCs) in our Galaxy are complex and highly structured, with broad, nonthermal line widths suggesting substantial turbulent motion (Falgarone & Philips 1990; Williams et al. 2000). Thus, MCs very likely are not static entities and might not necessarily be in an equilibrium state, but their properties could well be determined by their formation process. The importance of initial conditions for cloud structure is emphasized by observational and theoretical evidence for short cloud lifetimes (Ballesteros-Paredes et al. 1999; Elmegreen 2000; Hartmann et al. 2001; Hartmann 2002).

Flows are ubiquitous in the interstellar medium (ISM) due to the energy input by stars—photoionization, winds, and supernovae. In principle, they can pile up atomic gas to form MCs. Shock waves propagating into the warm ISM will fragment in the presence of thermal instability and linear perturbations (Koyama & Inutsuka 2000, 2002; Inutsuka & Koyama 2004; Hennebelle & Pérault 1999, 2000) and allow H_2 formation within a few megayears (Bergin et al. 2004) in a plane-parallel geometry. We envisage the colliding flows less as, e.g., interacting shells, but as (more or less) coherent gas streams from turbulent motions on scales of the order of the Galactic gaseous disk height (Ballesteros-Paredes et al.1999; Hartmann et al.2001). Parametrizing the inflows as a ram pressure allowed Hennebelle et al. (2003, 2004) to study the fragmentation and collapse of an externally pressurized slab.

In this Letter we present a study of the generation of filaments and turbulence in atomic clouds (which may be precursors of MCs) as a consequence of their formation process, extending the model of large-scale colliding H I flows outlined by Ballesteros-Paredes et al. (1999) and Burkert (2004; see also Audit & Hennebelle 2005). We discuss the dominant dynamical and thermal instabilities leading to turbulent flows and fragmentation of an initially completely uniform flow. Resulting nonthermal line widths in the cold gas (the progenitors of MCs) reproduce observed values, emphasizing the ease with which turbulent and filamentary structures can be formed in the ISM.

This study is a"proof of concept," discussing the dominant instabilities leading to nonlinear density perturbations. Since turbulence is thought to be one of the main agents controlling star formation (Larson 1981; Mac Low & Klessen 2004; Elmegreen & Scalo 2004), and consequent density fluctuations are surely crucial to gravitational fragmentation, star formation theory can benefit from a better understanding of the structure initially present in MCs. Detailed aspects and parameter studies will be presented in a forthcoming paper (F. Heitsch et al. 2005, in preparation).

2. PHYSICAL MECHANISMS

We restricted the models to hydrodynamics including thermal instabilities, leaving out the effects of gravity and magnetic fields. Gravity would lead to further fragmentation, and magnetic fields could have a stabilizing effect. For this regime, then, we identify three relevant instabilities:

1. The nonlinear thin shell instability (NTSI; Vishniac 1994) arises in a shock-bounded slab when ripples in a two-dimensional slab focus incoming shocked material and produce density fluctuations. The growth rate is $\sim c_s k(k\Delta)^{1/2}$, where c_s is the sound speed, k is the wavenumber along the slab, and Δ is the amplitude of the spatial perturbation of the slab. Numerical studies focused on the generation of substructure via Kelvin-Helmholtz modes (Blondin & Marks 1996), on the role of gravity (Hunter et al. 1986), and on the effect of the cooling strength (Hueckstaedt 2003). Walder & Folini (1998); and Walder & Folini (2000) discussed the interaction of stellar winds, and Klein & Woods (1998) investigated cloud collisions. The latter authors included magnetic fields, albeit only partially.

2. The flows deflected at the slab will cause Kelvin-Helmholtz instabilities (KHI), which have been studied at great length. For a step function profile in the velocity and constant densities across the shear layer, the growth rate is given by the velocity difference $k\Delta U$. If aligned with the flow, magnetic tension forces can stabilize against the KHI.

3. The thermal instability (TI; Field 1965) rests on the balancing of heating and cooling processes in the ISM. The TI develops an isobaric condensation mode and an acoustic mode,

[1] University Observatory Munich, Scheinerstrasse 1, 81679 Munich, Germany.
[2] University of Wisconsin–Madison, 475 North Charter Street, Madison, WI 53706.
[3] Harvard-Smithsonian Center for Astrophysics, 60 Garden Street, MS 42, Cambridge, MA 02138.
[4] Centre de Recherche Astronomique de Lyon, Ecole Normale Superieure, 69364, Lyon, Cedex 07, France.
[5] Centre de Recherche Astronomique de Lyon, Observatoire de Lyon 9, Avenue Charles Andre, 69561 Saint-Genis Laval Cedex, France.

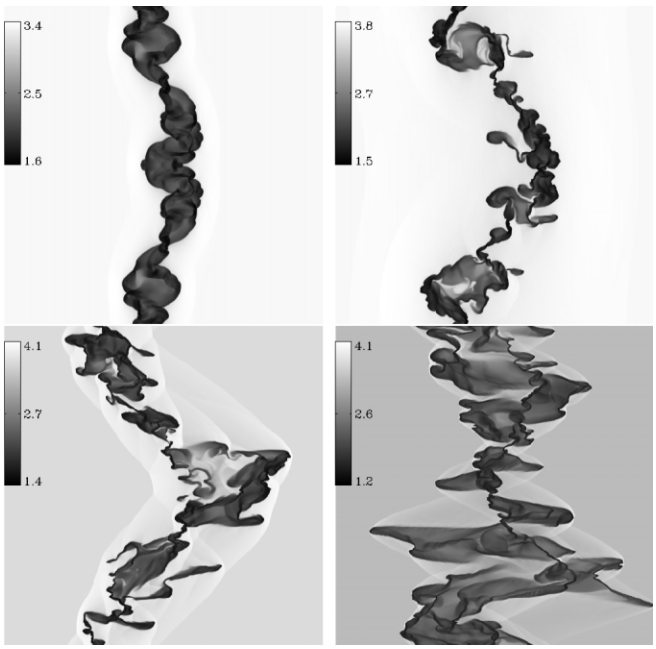

FIG. 1.—Temperature maps (log T in K) for models representative of the dominating instability (see text). From upper left to lower right: B1 (TI), C1 (KHI), C2, (KHI+NTSI), B3 (NTSI). Shown are models with 512^2 grid cells. [*See the electronic edition of the Journal for a color version of this figure*.]

which, under ISM conditions, is mostly damped. The condensation mode's growth rate is independent of the wave length, however, since it is an isobaric mode, smaller perturbations will grow first (Burkert & Lin 2000). A lower growth scale is set by heat conduction, whose scale needs to be resolved (Koyama & Inutsuka 2004). The signature of the TI are fragmentation and clumping as long as the sound crossing time is smaller than the cooling time scale. The TI can drive turbulence in an otherwise quiescent medium, even continuously, if an episodic heating source is available (Kritsuk & Norman 2002a; Kritsuk & Norman 2002b).

3. NUMERICAL METHOD

All three instabilities grow fastest (or at least first) on the smallest scales. This poses a dire challenge for the numerical method. We chose a method based on the second-order Bhatnagar-Gross-Krook (BGK) formalism (Prendergast & Xu 1993; Slyz & Prendergast 1999; Heitsch et al. 2004; Slyz et al. 2005), allowing control of viscosity and heat conduction. The statistical properties of the models are resolved with respect to grid resolution, viscosity, and heat conduction, although the flow patterns change in detail—as to be expected in a turbulent environment (F. Heitsch et al. 2005, in preparation). The linear resolution varies between 512 and 2048 cells. The heating and cooling rates are restricted to optically thin atomic lines following Wolfire et al. (1995), so that we are able to study the precursors of MCs up to the point when they could form H_2. Dust extinction becomes important above column densities of $N(\mathrm{H\,I}) \approx 1.2 \times 10^{21}$ cm^{-2}, which are reached only in the densest regions modeled. Thus, we use the unattenuated UV radiation field for grain heating (Wolfire et al. 1995), expecting substantial uncertainties in cooling rates only for the densest regions. The ionization degree is derived from a balance between ionization by cosmic rays and recombination, assuming that Lyα photons are directly reabsorbed.

Two opposing, uniform, identical flows in the x-y computational plane initially collide head-on at a sinusoidal interface with wave number $k_y = 1$ and amplitude Δ. The incoming flows are in thermal equilibrium. The system is thermally unstable for densities 1 cm $\lesssim n \lesssim$ 10 cm^{-3}. The cooling curve covers a density range of 10^{-2} cm $\leq n \leq 10^3$ cm^{-3} and a temperature range of 30 K $\leq T \leq 1.8 \times 10^4$ K. The box side length is 44 pc. Thus, Coriolis forces from Galactic rotation are negligible. For an interface with $\Delta = 0$, a cold high-density slab devoid of inner structure would form. The onset of the dynamical instabilities thus can be controlled by varying the amplitude of the interface perturbation. This allows us to test turbulence generation under minimally favorable conditions.

Model series B has $n_0 = 1.0$ cm^{-3} and $T_0 = 2.5 \times 10^3$ K; series C has $n_0 = 0.5$ cm^{-3} and $T_0 = 5.3 \times 10^3$ K. The amplitude of the interface perturbation corresponds to 2.5% of the box length, i.e., 1.1 pc in the horizontal direction. The second digit of the model name gives the Mach number of the inflow. The inflow velocity varies in the range 6 km s^{-1} $< v_{\mathrm{in}} <$ 17 km s^{-1}.

4. RESULTS

We choose to present a few models containing the salient features of cloud formation via colliding flows. We ask how hard it is to generate nonlinear turbulent density perturbations in an otherwise uniform flow.

4.1. *Dominant Instabilities*

The structures generated in colliding flows depend strongly on the initial parameters (Fig. 1),[6] as a result of the dominating instability. This is not surprising, since all three instabilities at work have different signatures. For high-density, low-velocity inflows (model B1, *upper left*), the TI dominates and leads to fast cooling, manifested in a coherent slab of cold gas. This situation comes closest to the one-dimensional plane-parallel slab.

Reducing the density (model C1; Fig. 1, *upper right*) leads to less efficient cooling, thus giving the dynamical instabilities time to work, here dominated by the KHI. The eddies are visible at the flanks of the initial slab. For higher inflow speeds the vertical x momentum transport increases, so that for model C2 (*lower left*), the NTSI will arise. Its typical signature are long strands of denser gas predominantly along the flow direction (Hueckstaedt 2003). The KHI modes that are still discernible here have vanished in model B3. There, the NTSI dominates the dynamics almost completely. Oblique flows (not shown) lead to a nearly instantaneous breakup of the initial slab, because they excite KHI modes at the scale of the initial, nonlinear perturbation. We ran models up to Mach 4, up to which the NTSI dominates more and more with higher Mach number. This morphological discussion will be quantified in subsequent work.

Despite the symmetric initial conditions, all models develop large-scale asymmetries well after the onset of the instabilities and the growth of turbulent structures, i.e., in the nonlinear phase. For adiabatic or isothermal test cases as well as for one-dimensional problems including cooling, the code preserves perfect symmetry.

4.2. *Mass Distribution*

Figure 2 shows the mass spectrum of cores. Cores are defined as coherent regions with densities $n > 100$ cm^{-3}. Each of the histograms comprises approximately 50 cores. The dashed line denotes a spectral index of -1.7, as observed for molecular cores

[6] All plots without time dependence are taken at the end point of the corresponding model, i.e., at 15 Myr for model B3, and at 19 Myr for all other models.

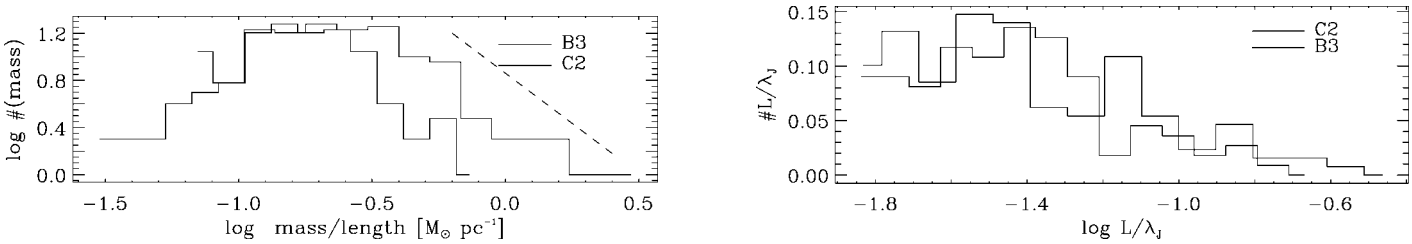

FIG. 2.—*Left:* Mass histogram of likely precursors of molecular clouds, with densities $n > 100$ cm^{-3} (C2 and B3). The dashed line denotes a power law with exponent -1.7. The resolution limit is $M_r = 1.8\ M_\odot$ pc^{-1}. *Right:* Histogram of the local Jeans number L/λ_J for the precursors (models C2 and B3). None of the dense objects would be gravitationally bound.

(Heithausen et al. 1998). The resolution limit for both histograms lies at $1.8\ M_\odot$ pc^{-1}. Note that (1) these "cores" correspond to cold H I regions, not molecular cores, and that (2) the masses are per length in our two-dimensional models. A direct comparison between these two-dimensional spectra and observed three-dimensional mass spectra requires assumptions concerning what structures the filaments would correspond to in three dimensions. If the probability density functions are the same for two dimensions and three dimensions, the mass spectra are expected to be flatter in three dimensions (Chappell & Scalo 2001).

Would the cores be gravitationally unstable? Although the models do not include self-gravity, we can estimate the thermal Jeans length $\lambda_J \equiv [\pi/(G\rho)]^{1/2} c_s$ and its turbulent counterpart $\lambda_t \equiv [\pi/(G\rho)]^{1/2}\langle v^2\rangle^{1/2}$. The ratio of the core's size over the core's Jeans length is $n_J \equiv L/\lambda_J < 1$, meaning none of the cores would be gravitationally unstable (Fig. 2; *right*). Since $\lambda_J \propto T^{1/2}/(P/T)^{1/2} \propto T$ for an isobaric contraction, the histogram of Figure 2 (*right*) would shift by a factor of 3 to larger Jeans masses if we cooled the gas down to $T \approx 10$ K, thus still yielding Jeans-stable objects. The core size is determined by the geometric mean of the longest and shortest radius.

However, determining the "global" Jeans number of the cold gas—given by the thickness of the slab over the global Jeans length derived from the mean density and temperature in the cold gas—after 10 Myr for model B3 and 15 Myr for model C2, the length scale of the cold gas $L > \lambda_J$, i.e., the "slab" would become gravitationally unstable without turbulence (Fig. 3). These quantities are global measures in the sense that they do not refer to isolated cold regions. The turbulent Jeans length $\lambda_t > L$ for all times and models. Global (i.e., large-scale) gravitational effects could still have a crucial effect on the system (Burkert & Hartmann 2004), especially once the inflow stops.

4.3. *Line Widths and Kinetic Energy Modes*

MCs consistently show nonthermal line widths of a few kilometers per second, that, together with temperatures of $T \approx 10$ K, are generally interpreted as supersonic turbulence. The line widths in our models are consistent with the observed values (Fig. 4). The "observed" line width is derived from the density-weighted histogram of the line-of-sight velocity dispersion in the cold gas at $T < 100$ K (*filled symbols*). Since the *internal* line width of coherent cold regions (*open symbols*) range around the sound speed of the cold gas (0.8 km s^{-1}), the internal velocity dispersions do not reach Mach numbers $\mathcal{M} > 1$. Hence, the "supersonic" line widths are a consequence of cold regions moving with respect to each other but are not a result of internal supersonic turbulence in the cold gas that eventually would be hosting star formation. Hartmann (2002) argues that, because of the ages and small spatial dispersions of young stars in Taurus, their velocity dispersions relative to their natal gas are very likely subsonic. The turbulent line widths amount only to a fraction of the inflow velocity.

Figure 5 shows the compressible, the solenoidal and the total specific kinetic energy for the whole domain (*left*) and for the cold gas ($T < 100$ K; *right*). Compressible modes dominate the total specific kinetic energy because of the large-scale colliding flows. However, within the bounding shocks, the highly compressible inflows are converted into solenoidal motions by a combination of thermal and dynamical instabilities (see Kritsuk & Norman 2004). Because of the two-dimensional geometry, the ratio of solenoidal over compressible kinetic energy is only a lower limit. An extension of Figure 5 to radiative losses allows us to estimate the overall efficiency of turbulence generation in MCs.

5. SUMMARY

Even for completely uniform inflows, we have shown that the combination of dynamical and thermal instabilities efficiently generates nonlinear density perturbations that seed structure of eventual MCs. There is a direct correlation between the morphology of the resulting clouds and the dominating instability.

While our "cloud" would be gravitationally unstable, the isolated cold regions would still be stabilized against gravity by thermal pressure. However, fragmentation and turbulent

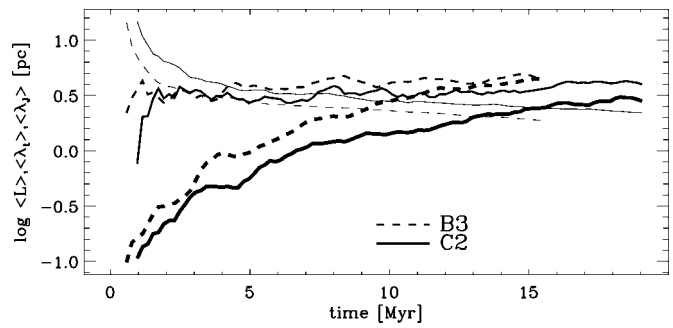

FIG. 3.—Average length scale (*thick lines*), turbulent Jeans length (*medium lines*), and thermal Jeans length (*thin lines*) for models C2 and B3 vs. time.

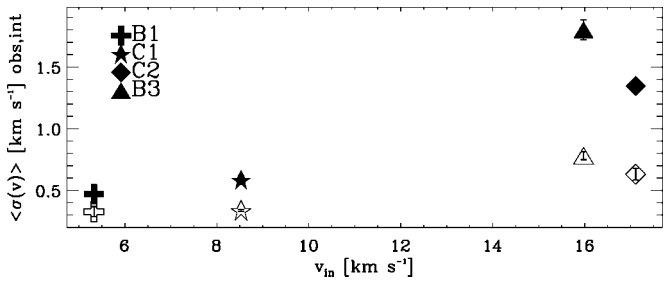

FIG. 4.—Mean velocity dispersion in cold gas at $T < 100$ K (*filled symbols*) and in cold coherent regions (*open symbols*) vs. the inflow velocity.

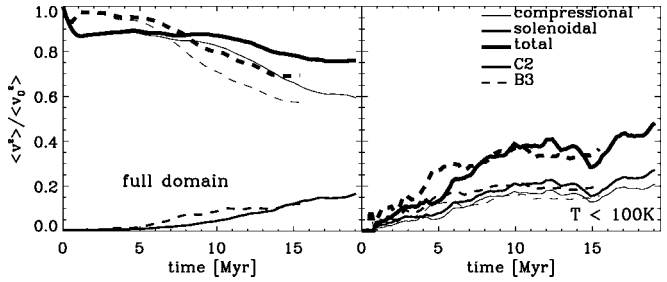

FIG. 5.—Specific kinetic energy fraction against time for models C2 and B3, split up into compressional, solenoidal, and total specific kinetic energy, for the whole domain (*left*) and for cold gas ($T < 100$ K; *right*). The specific kinetic energy is normalized to the value at $t = 0$.

mixing driven by the incoming warm gas also would prevent the global collapse of the cloud, with the caveat that a finite extent of the cloud in the vertical direction might lead to edge effects resulting in collapse (Burkert & Hartmann 2004). Line widths reached in the cold gas are consistent with observed values of a few kilometers per second—only a fraction of the inflow speed. The internal line widths, however, are generally subsonic. While the line widths are "supersonic" with respect to the cold gas, this is not necessarily a hydrodynamically accurate description of the cold gas.

Although we set the physical regime for our models by adopting a cooling curve, we expect the mechanism to work on a variety of scales. The surface density of the cold gas should give us a rough estimate of the amount of stars forming later on. Even though the cold gas mass depends strongly on the turbulent evolution of the slab, it correlates strongly with the inflow momentum. In this sense, colliding flows not only could explain the rather quiescent star formation events as in Taurus, but would be a suitable model for generating star bursts in galaxy mergers.

We enjoyed the discussions with J. Gallagher, L. Sparke, and E. Zweibel. We thank the referee for a very constructive report. Computations were performed on Ariadne built by S. Jansen at UW-Madison, and at the NCSA (AST-040026). This work was supported by the NSF (AST-0328821).

REFERENCES

Audit, E., & Hennebell, P. 2005, A&A, 433, 1
Ballesteros-Paredes, J., Hartmann, L., & Vázquez-Semadeni, E. 1999, ApJ, 527, 285
Bergin, E. A., Hartmann, L. W., Raymond, J. C., & Ballesteros-Paredes, J. 2004, ApJ, 612, 921
Blondin, J. M., & Marks, B. S. 1996, NewA, 1, 235
Burkert, A. 2004, in ASP Conf. Ser. 322: The Formation and Evolution of Massive Young Star Clusters, ed. H. J. G. L. M. Lamers, L. J. Smith, & A. Nota (San Francisco: ASP), 489
Burkert, A., & Hartmann, L. 2004, ApJ, 616, 288
Burkert, A., & Lin, D. N. C. 2000, ApJ, 537, 270
Chappell, D., & Scalo, S. 2001, MNRAS, 325, 1
Elmegreen, B. G. 2000, ApJ, 530, 277
Elmegreen, B. G., & Scalo, J. 2004, ARA&A, 42, 211
Falgarone, E., & Philips, T. G. 1990, ApJ, 359, 344
Field, G. B. 1965, ApJ, 142, 531
Hartmann, L. 2002, ApJ, 578, 914
Hartmann, L., Ballesteros-Paredes, J., & Bergin, E. A. 2001, ApJ, 562, 852
Heithausen, A., Bensch, F., Stutzki, J., Falgarone, E., & Panis, J. F. 1998, A&A, 331, L65
Heitsch, F., Zweibel, E. G., Slyz, A. D., & Devriendt, J. E. G. 2004, ApJ, 603, 165
Hennebelle, P., & Pérault, M. 1999, A&A, 351, 309
———. 2000, A&A, 359, 1124
Hennebelle, P., Whitworth, A. P., Cha, S.-H., & Goodwin, S. P. 2004, MNRAS, 348, 687
Hennebelle, P., Whitworth, A. P., Gladwin, P. P., & André, P. 2003, MNRAS, 340, 870
Hueckstaedt, R. M. 2003, NewA, 8, 295
Hunter, J. H., Jr., Sandford, M. T., II, Whitaker, R., & Klein, R. I. 1986, ApJ, 305, 309
Inutsuka, S., & Koyama, H. 2004, Rev. Mex. AA, 22, 26
Klein, R. I., & Woods, D. T. 1998, ApJ, 497, 777
Koyama, H., & Inutsuka, S. 2000, ApJ, 532, 980
———. 2002, ApJ, 564, L97
———. 2004, ApJ, 602, L25
Kritsuk, A. G., & Norman, M. L. 2002a, ApJ, 569, L127
———. 2002b, ApJ, 580, L51
———. 2004, ApJ, 601, L55
Larson, R. B. 1981, MNRAS, 194, 809
Mac Low, M.-M., & Klessen, R. S. 2004, Rev. Mod. Phys., 76, 125
Prendergast, K. H., & Xu, K. 1993, J. Comput. Phys., 109, 53
Slyz, A. D., Devriendt, J. E. G., Bryan, G., & Silk, J. 2005, MNRAS, 356, 737
Slyz, A. D., & Prendergast, K. H. 1999, A&AS, 139, 199
Vishniac, E. T. 1994, ApJ, 428, 186
Walder, R., Folini, D. 1998, Ap&SS, 260, 215
———. 2000, Ap&SS, 274, 343
Williams, J. P., Blitz, L., & McKee, C. F. 2000, in Protostars and Planets IV, ed. V. Manning, A. P. Boss, & S. S. Russell (Tucson: Univ. Arizona Press), 97
Wolfire, M. G., Hollenbach, D., McKee, C. F., Tielens, A. G. G. M., & Bakes, E. L. O. 1995, ApJ, 443, 152